UNITED
NATIONS

EP

United Nations
Environment
Programme

UNEP (DEPI)/RS.12 /7

Original: ENGLISH

12th Global Meeting of the Regional Seas Conventions and Action Plans

Bergen, Norway, 20th – 22nd September 2010

Coastal Ecosystem–Based Management with Nonlinear Ecological Functions and Values

Coastal Ecosystem-Based Management with Nonlinear Ecological Functions and Values

Edward B. Barbier, *et al.*

Science **319**, 321 (2008);
DOI: 10.1126/science.1150349

Science (print ISSN 0036-8075; online ISSN 1095-9203) is published weekly, except the last week in December, by the American Association for the Advancement of Science, 1200 New York Avenue NW, Washington, DC 20005.

Coastal Ecosystem–Based Management with Nonlinear Ecological Functions and Values

Edward B. Barbier,[1]* Evamaria W. Koch,[2] Brian R. Silliman,[3] Sally D. Hacker,[4] Eric Wolanski,[5] Jurgenne Primavera,[6] Elise F. Granek,[7] Stephen Polasky,[8] Shankar Aswani,[9] Lori A. Cramer,[10] David M. Stoms,[11] Chris J. Kennedy,[1] David Bael,[8] Carrie V. Kappel,[12] Gerardo M. E. Perillo,[13] Denise J. Reed[14]

A common assumption is that ecosystem services respond linearly to changes in habitat size. This assumption leads frequently to an "all or none" choice of either preserving coastal habitats or converting them to human use. However, our survey of wave attenuation data from field studies of mangroves, salt marshes, seagrass beds, nearshore coral reefs, and sand dunes reveals that these relationships are rarely linear. By incorporating nonlinear wave attenuation in estimating coastal protection values of mangroves in Thailand, we show that the optimal land use option may instead be the integration of development and conservation consistent with ecosystem-based management goals. This result suggests that reconciling competing demands on coastal habitats should not always result in stark preservation-versus-conversion choices.

More than one-third of the world's human population lives in coastal areas and small islands (*1*), which together make up just 4% of Earth's total land area. Coastal population densities are nearly three times that of inland areas (*2*) and they are increasing exponentially. The long-term sustainability of these populations is dependent on coastal ecosystems and the services they provide, such as storm buffering, fisheries production, and enhanced water quality. Despite the importance of these services, degradation and loss of coastal ecosystems over the past two to three decades—including marshes (50% either lost or degraded), mangroves (35%), and reefs (30%)—is intense and increasing worldwide (*2*–*4*).

To aid in conservation of these coastal communities, ecosystem-based management (EBM) has recently been proposed as a benefit optimization and decision-making strategy that incorporates often conflicting development and conservation uses (*5*–*7*). EBM strives to reconcile these pressures by valuing ecosystem services and thus justifying the maintenance of many natural systems "in healthy, productive and resilient conditions so that they can provide the services humans want and need" (*5*). Yet the implementation of EBM cannot take place without addressing a fundamental challenge: assessing the true value of these ecosystems and the services they generate, so that practical compromises can be made (*8*–*11*).

The interrelationship of ecosystem structure, function, and economic value is critical to coastal management decisions, which are often concerned with how much natural habitat to "preserve" and how much to allocate to human development activities (*2*, *3*). In assessing such trade-offs, it is frequently assumed that ecosystem services change linearly with critical habitat variables such as size (e.g., area). This assumption can lead to the misrepresentation of economic values inherent in services, particularly at their endpoints. The endpoint values often either overestimate or underestimate the service value, resulting in an "all or none" habitat scenario as the only decision choice (*9*–*11*). A common reason for invoking such an assumption is that few data exist for examining the marginal losses associated with changes in nonlinear ecological functions, making

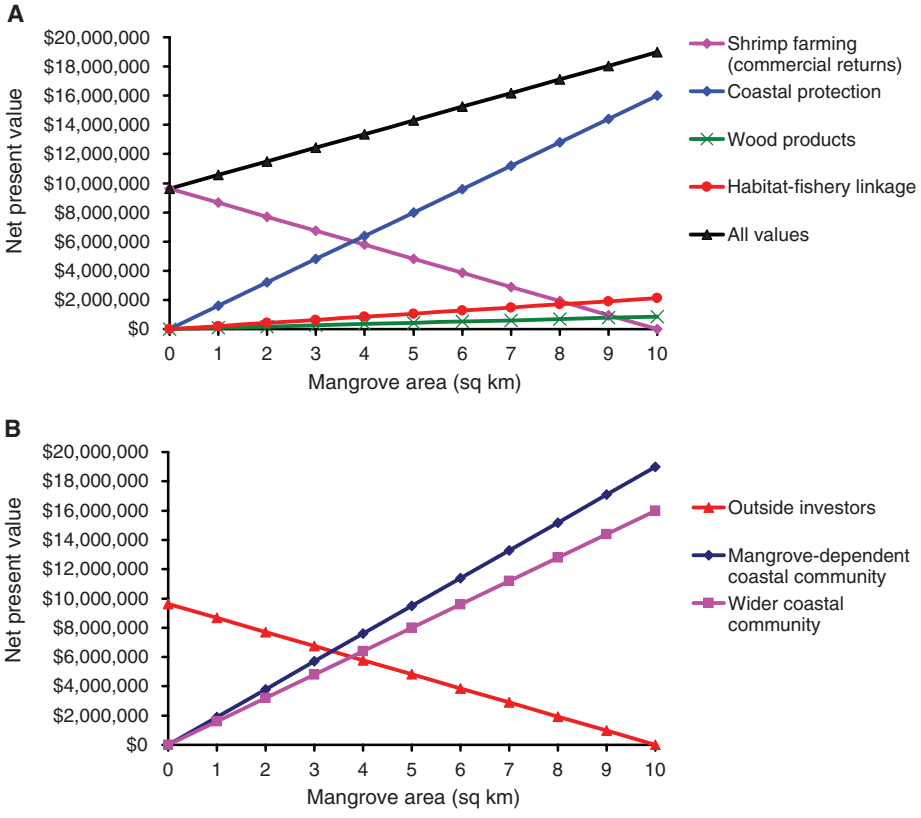

Fig. 1. Conventional comparison of shrimp farming to various mangrove services at coastal landscape level (10 km^2), Thailand (net present value, 10% discount rate, 1996 dollars) on the basis of (**A**) total economic returns as a function of mangrove area (km^2) for the commercial returns from shrimp farming plus three mangrove ecosystem service values: coastal protection, wood product collection, and habitat support for offshore fisheries; and (**B**) the distribution of benefits as a function of mangrove area (km^2) among three stakeholders: outside investors in shrimp farms, the mangrove-dependent coastal community, and the wider coastal community (up to 5 km away). [Based on data from (*11*, *16*, *17*)]

[1]Department of Economics and Finance, University of Wyoming, Laramie, WY 82071, USA. [2]Horn Point Laboratory, University of Maryland Center for Environmental Science, Cambridge, MD 21613, USA. [3]Department of Zoology, University of Florida, Gainesville, FL 32611, USA. [4]Department of Zoology, Oregon State University, Corvallis, OR 97331, USA. [5]Australian Centre for Tropical Freshwater Research, James Cook University and Australian Institute of Marine Science, Townsville, Queensland 4810, Australia. [6]Aquaculture Department, Southeast Asian Fisheries Development Center, Tigbauan, Iloilo 5021, Philippines. [7]Environmental Sciences and Resources, Portland State University, Portland, OR 97207, USA. [8]Department of Applied Economics, University of Minnesota, St. Paul, MN 55108, USA. [9]Department of Anthropology, University of California, Santa Barbara, CA 93106, USA. [10]Department of Sociology, Oregon State University, Corvallis, OR 97331, USA. [11]Bren School of Environmental Science and Management, University of California, Santa Barbara, CA 93106, USA. [12]National Center for Ecological Analysis and Synthesis, University of California, Santa Barbara, CA 93101, USA. [13]Instituto Argentino de Oceanografía, B8000FWB Bahía Blanca, Argentina. [14]Department of Earth and Environmental Sciences, University of New Orleans, New Orleans, LA 70148, USA.

*To whom correspondence should be addressed. E-mail: ebarbier@uwyo.edu

it difficult to value accurately the changes in ecosystem services in response to incremental changes in habitat characteristics (e.g., area). If, however, relationships between the structure and function of coastal habitats are nonlinear, as ecological theory suggests (*12*–*14*), then assuming that the value of the resulting service is linear (with respect to changes in habitat characteristics) will mislead management decisions.

To test the key assumption that ecosystem services and their economic value are linearly related to habitat area, we used data collected in the field from key coastal interface systems around the globe, including mangroves, salt marshes, seagrass beds, nearshore coral reefs, and sand dunes (*15*). We focused on arguably the most undervalued ecosystem service until recently: protection against wave damage caused by storms, hurricanes, and tsunamis. These field data reveal that for all these coastal habitats, nonlinear relationships exist between habitat area and measurements of the ecosystem function of wave attenuation (fig. S1). For mangroves and salt marshes, there are quadratic and exponential decreases, respectively, in wave height with increasing habitat distance inland from the shoreline (fig. S1, A and B). In the case of seagrasses and nearshore coral reefs, wave attenuation is a function of the water depth above the grass bed or reef, and these relationships are also nonlinear (fig. S1, C and D). Additionally, there is an exponential relationship between the percent cover of dune grasses and the size of oceanic waves blocked by sand dunes produced by the grass (fig. S1E). These data suggest that the assumption of linearity is likely to be inaccurate for many ecosystem services that depend on habitat size—a result that could have important implications for conservation, especially as it relates to EBM.

To explore this possibility, we applied these nonlinear wave attenuation relationships for coastal systems to a case study from Thailand (*11*, *16*, *17*) where choices have been made between conversion of mangroves to shrimp aquaculture versus their preservation for key ecosystem services (such as coastal protection and fish habitat). Our case study assumes a mangrove habitat that extends 1000 m inland from the seaward edge along 10 km of coast. Nearby communities depend on the mangrove for forest and fishery products in coastal waters that are populated by mangrove-dependent fish. Coastal communities up to 5 km inland are protected from tropical storms by mangroves. The alternative to preserving mangroves is converting them to intensive shrimp ponds, which overwhelmingly benefits outside investors (*11*, *16*, *17*).

Figure 1A depicts the economic returns from converting the 10-km^2 mangrove habitat to commercial shrimp farms as well as the values generated by three ecosystem services: coastal protection, wood collection, and habitat-fishery linkage. The figure also aggregates all four values to test whether an "integrated" land use option involving some conversion and some preservation yields the highest total value. When all values are linear, the outcome is a typical "all or none" scenario; either the aggregate values will favor complete conversion, or they will favor preserving the entire habitat (Fig. 1A). Because the ecosystem service values are large and increase linearly with mangrove area, the preservation option is preferred (Fig. 1A). The aggregate value of the mangrove system is at its highest ($18.98 million) when it is completely preserved, and any conversion to shrimp farming would lead to less aggregate value compared to full preservation. Thus, an EBM strategy that considers all the values of the ecosystem would favor mangrove preservation and no shrimp farm conversion.

Figure 1B shows that mangrove-dependent communities and the wider coastal community would benefit from the EBM decision, whereas outside investors would prefer conversion of the mangrove to shrimp ponds. Overall, our analysis shows that the EBM strategy of full preservation of the mangroves would face opposition from outside investors, who would obtain no commercial gains from this scenario but would make profits of more than $9.6 million from complete conversion (Fig. 1B). It is also clear that the "all or none" decision to preserve mangroves hinges on the coastal protection value service of the mangroves, which is assumed to increase linearly with mangrove area.

However, if we consider that coastal protection afforded by mangroves depends on their functional ability to attenuate storm waves (*18*–*21*) and that this relationship is nonlinear (fig. S1A), a different EBM strategy is supported (Fig. 2). In fig. S1A, we show that a wave height of 1.1 m at the offshore edge of the mangrove forest would be reduced to 0.91 m if the forest extended 100 m inland; if the forest extended 200 m inland, the wave would drop to roughly 0.75 m. The wave would continue to fall, albeit at a declining rate, for every additional 100 m of mangroves inland from the sea. For a forest extending 1000 m inland, the wave would be reduced to a negligible 0.12 m.

Using the nonlinear wave attenuation function for mangroves (fig. S1A), it is possible to revise the estimate of storm protection service value for the Thailand case study (*22*) (Fig. 2). The storm protection service of mangroves still dominates all values, but small losses in mangroves will not cause the economic benefits of storm buffering by mangroves to fall precipitously (Fig. 2A). The consequence is that the aggregate value across all uses of the mangroves (i.e., shrimp farming and ecosystem values) is at

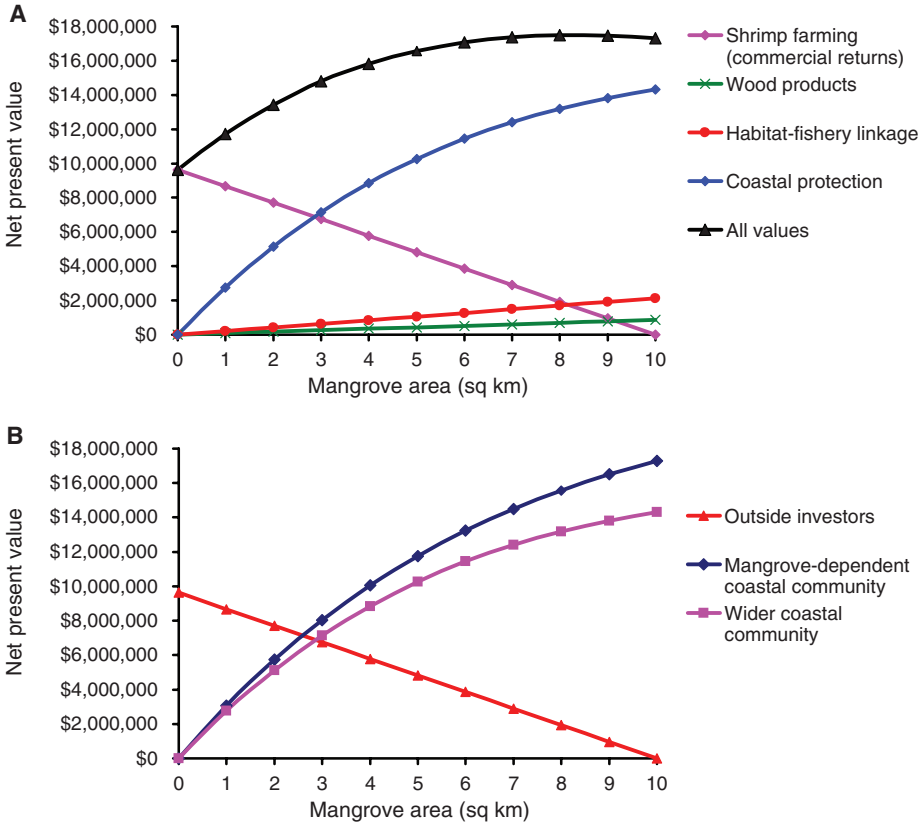

Fig. 2. Alternative comparison of shrimp farming to various mangrove services at coastal landscape level (10 km^2), Thailand (calculated as in Fig. 1), incorporating the nonlinear wave attenuation function from fig. S1A, on the basis of (**A**) total economic returns as a function of mangrove area (km^2) for the commercial returns from shrimp farming plus three mangrove ecosystem service values: coastal protection, wood product collection, and habitat support for offshore fisheries; and (**B**) the distribution of benefits as a function of mangrove area (km^2) among three stakeholders: outside investors in shrimp farms, the mangrove-dependent coastal community, and the wider coastal community (up to 5 km away).

its highest ($17.5 million) when up to 2 km^2 of mangroves are allowed to be converted to shrimp aquaculture and the remainder of the ecosystem is preserved. This outcome also yields a more equitable distribution across stakeholders (Fig. 2B), which may be an important objective in any EBM strategy for coastal management. Local mangrove-dependent coastal communities and other coastal communities living within 5 km inland would obtain approximately the same share of economic benefits from the mangrove system ($15.6 and $13.2 million, respectively), but now outside investors would earn some commercial profits from shrimp farming ($1.9 million). Finally, we note that the outcome from our Thailand mangrove valuation example corresponds to "best practice" guidelines for mangrove management in Asia, which recommend that ideal mangrove/pond ratios should not exceed 20% of the habitat area converted to ponds (*23*, *24*).

By including nonlinear relationships in an economic valuation of ecosystem services, our results challenge the assumption that the competing demands of coastal interface systems must always result in either conservation or habitat destruction. As the case study of Thailand mangroves illustrates, the way in which ecological and economic analysis is combined to estimate the values of various ecosystem services can have a large impact on coastal EBM outcome. If point estimates of these values are used to project linear relationships between the benefits of ecosystem services with respect to changes in key ecosystem physical attributes, such as area or distance from shore, then the result might be to force EBM decision-making into a simple "all or none" choice. This result is at odds with EBM strategies, which emphasize reconciliation between economic development pressures and conservation of critical ecosystem resources and services (*5*–*8*). However, if the nonlinear ecological function underlying a service, such as coastal protection afforded by mangroves, is incorporated into economic valuation, then we more realistically represent how ecosystem services change with habitat conversion and how EBM may best be used.

References and Notes

1. Coastal areas are defined in (*2*, *3*) as habitat from the low water mark (<50 m depth) to the coastline and inland from the coastline to a maximum of 100 km or 50-m elevation (whichever is closer to the sea).
2. *Marine and Coastal Ecosystems and Human Well-Being: A Synthesis Report Based on the Findings of the Millennium Ecosystem Assessment* (UN Environment Programme, Nairobi, 2006).
3. Millennium Ecosystem Assessment, *Ecosystems and Human Well-Being: Current State and Trends* (Island, Washington, DC, 2005), chap. 19.
4. I. Valiela, J. Bowen, J. York, *Bioscience* **51**, 807 (2001).
5. K. McLeod, J. Lubchenco, S. Palumbi, A. Rosenberg, Scientific Consensus Statement on Marine Ecosystem-Based Management (Communication Partnership for Science and the Sea, 2005; http://compassonline.org/marinescience/solutions_ecosystem.asp).
6. T.-E. Chua, D. Bonga, N. Bermas-Atrigenio, *Coast. Manage.* **34**, 303 (2006).
7. *Ecosystem-Based Management: Markers for Assessing Progress* (UN Environment Programme/GPA, The Hague, 2006).
8. P. Kareiva, S. Watts, R. McDonald, T. Boucher, *Science* **316**, 1866 (2007).
9. A. Balmford *et al*., *Science* **297**, 950 (2002).
10. L. Brander, R. Florax, J. Vermaat, *Environ. Resour. Econ.* **33**, 223 (2006).
11. E. Barbier, *Econ. Policy* **22**, 177 (2007).
12. K. Gaston, T. Blackborn, *Pattern and Process in Macroecology* (Blackwell Science, Oxford, ed. 2, 2000).
13. J. Petersen *et al*., *Bioscience* **53**, 1181 (2003).
14. E. Farnsworth, *Global Ecol. Biogeogr. Lett.* **7**, 15 (1998).
15. See supporting material on *Science* Online.
16. E. Barbier, *Contemp. Econ. Policy* **21**, 59 (2003).
17. S. Sathirathai, E. Barbier, *Contemp. Econ. Policy* **19**, 109 (2001).
18. S. Massel, K. Furukawa, R. Brinkman, *Fluid Dyn. Res.* **24**, 219 (1999).
19. Y. Mazda, M. Magi, M. Kogo, P. N. Hong, *Mangroves Salt Marshes* **1**, 127 (1997).
20. Y. Mazda, M. Magi, Y. Ikeda, T. Kurokawa, T. Asano, *Wetlands Ecol. Manage.* **14**, 365 (2006).
21. E. Wolanski, in *Coastal Protection in the Aftermath of the Indian Ocean Tsunami: What Role for Forests and Trees?*, S. Braatz, S. Fortuna, J. Broadhead, R. Leslie, Eds. (FAO, Bangkok, 2007), pp. 157–179.
22. The wave attenuation relationship of fig. S1A was transformed into percent wave reduction as a function of 100-m inland mangrove distance, and this relationship was used to adjust the net present value per km^2 estimate for storm protection used in Fig. 1A, assuming that each km^2 of mangroves deforested involved the equivalent loss of 100 m of mangroves inland along the 10-km coastline. See (*15*) for details.
23. P. Saenger, E. Hegerl, J. Davie, *Global Status of Mangrove Ecosystems* (IUCN, Gland, Switzerland, 1983).
24. J. Primavera *et al*., *Bull. Mar. Sci.* **80**, 795 (2007).

25. This work was conducted as part of the "Measuring ecological, economic, and social values of coastal habitats to inform ecosystem-based management of land-sea interfaces" Working Group supported by the National Center for Ecological Analysis and Synthesis, funded by NSF grant DEB-0553768; the University of California, Santa Barbara; the State of California; and the David and Lucile Packard Foundation. We thank B. Halpern for his assistance with this project and work, and three anonymous reviewers for their constructive comments.

Supporting Online Material

www.sciencemag.org/cgi/content/full/319/5861/321/DC1
Materials and Methods
Figs. S1 and S2
Tables S1 to S3
References

11 September 2007; accepted 22 November 2007
10.1126/science.1150349

β-Catenin Defines Head Versus Tail Identity During Planarian Regeneration and Homeostasis

Kyle A. Gurley, Jochen C. Rink, Alejandro Sánchez Alvarado*

After amputation, freshwater planarians properly regenerate a head or tail from the resulting anterior or posterior wound. The mechanisms that differentiate anterior from posterior and direct the replacement of the appropriate missing body parts are unknown. We found that in the planarian *Schmidtea mediterranea*, RNA interference (RNAi) of β-*catenin* or *dishevelled* causes the inappropriate regeneration of a head instead of a tail at posterior amputations. Conversely, RNAi of the β-catenin antagonist *adenomatous polyposis coli* results in the regeneration of a tail at anterior wounds. In addition, the silencing of β-*catenin* is sufficient to transform the tail of uncut adult animals into a head. We suggest that β-catenin functions as a molecular switch to specify and maintain anteroposterior identity during regeneration and homeostasis in planarians.

β-Catenin is a multifunctional protein that controls transcriptional output as well as cell adhesion. During embryonic development of both vertebrates and invertebrates, β-catenin regulates a variety of cellular processes, including organizer formation, cell fate specification, proliferation, and differentiation (*1*–*9*). In adult animals, the Wnt/β-catenin pathway participates in regeneration and tissue homeostasis; misregulation of this pathway can lead to degenerative diseases and cancer in humans (*9*–*12*). In response to upstream cues, such as Wnt ligands binding to Frizzled receptors, β-catenin accumulates in nuclei (Fig. 1A) and invokes transcriptional responses that direct the specification and patterning of tissues (*13*, *14*). Adenomatous polyposis coli (APC) is an essential member of a destruction complex that phosphorylates β-catenin, resulting in its constitutive degradation. Hence, loss of APC leads to a rise in β-catenin levels that is sufficient to drive transcriptional responses (*15*). The intracellular protein Dishevelled has multiple functions but plays an essential role as a positive regulator of β-catenin by inhibiting the destruction complex (*16*).

As part of a systematic effort to define the roles of signaling pathways in planaria, we analyzed the canonical Wnt signaling system in *Schmidtea mediterranea*. We cloned and determined the expression patterns of all identifiable homologs of core pathway components (Fig. 1A) and silenced them, individually or in combina-

Department of Neurobiology and Anatomy, Howard Hughes Medical Institute, University of Utah School of Medicine, 401 MREB, 20N 1900E, Salt Lake City, UT 84132, USA.

*To whom correspondence should be addressed. E-mail: sanchez@neuro.utah.edu

www.sciencemag.org/cgi/content/full/319/5861/321/DC1

Supporting Online Material for

Coastal Ecosystem–Based Management with Nonlinear Ecological Functions and Values

Edward B. Barbier,* Evamaria W. Koch, Brian R. Silliman, Sally D. Hacker, Eric Wolanski, Jurgenne Primavera, Elise F. Granek, Stephen Polasky, Shankar Aswani, Lori A. Cramer, David M. Stoms, Chris J. Kennedy, David Bael, Carrie V. Kappel, Gerardo M. E. Perillo, Denise J. Reed

*To whom correspondence should be addressed. E-mail: ebarbier@uwyo.edu

Published 18 January 2008, *Science* **319**, 321 (2008)
DOI: 10.1126/science.1150349

This PDF file includes:

The wave attenuation relationships based on field data for mangroves, salt marshes, seagrass beds, nearshore coral reefs, and sand dunes are displayed in Fig. S1 below. The materials and methods for describing each relationship depicted in the figure are as follows.

Fig. S1A <u>Mangrove</u>

Wave attenuation for mangroves is based on data from (*S1*) at the coast of Vietnam where *Kandelia candel* and *Sonneratia caseolaris* mangrove plantations have been created over a wide intertidal shoal as a coastal defense against typhoon waves. The *K. candel* plantation at the study site is 1.5 km wide (perpendicular to the coast) and 3 km long (parallel to the coast). Wave data was measured *in situ* at three locations: at the offshore edge of the forest (no attenuation by the vegetation), 100 m inside the forest, and approximately 1000m from the 1st sampling site.

RMD-type wave gauges (Rigosha et Co., Ltd) recorded water height at a 0.5 Hz frequency during one whole day (spring tide) with a 1.5 mm accuracy, during the passage of a typhoon offshore. The records were separated into two parts, the tidal elevation with a long period (12-24 hr) and the wind-induced random waves, i.e. the swells or long waves with short periods (ca 10 s period) by the running average method over 20 min. The significant wave height at the three sampling locations was calculated as the average of the highest one-third of the waves. Significant wave heights at other distances from the edge of the mangrove forest were then modeled based on wave theory using:

$$\frac{dH}{dx} = -rH$$

where H is the wave height ($H=H_0$ at $x=0$), x is the distance into the mangrove forest from the seaward edge, and r is the wave attenuation coefficient. The parameter r is a function of water depth and mangrove species (Table S1). Depth at the seaward edge of the mangrove forest was 1.5 m at high tide and 0.8 m at mid-tide. Depth at the landward side of the mangroves was 0.7 m less than that at the seaward edge. Depth was assumed to vary linearly with x and water level was assumed horizontal. Values of r per 100 m were between 17 and 60% (Table S1). The observed wave height of 1 m at the open sea was reduced to 0.05 m at the coast, enabling aquaculture ponds to exist behind a 2 m high coastal levee. Without the sheltering effect of mangroves the waves would arrive at the coast with wave height of 0.75 m and the weakly constructed levee could be eroded and possibly breached. Although the typhoon created a storm surge that flooded the levee, it survived and protected the ponds as swell/waves were negligible in the shadow of the mangroves. This is only possible when the forest itself is protected by a wide (5 km) intertidal shoal offshore of the mangrove forest that reduces the typhoon waves to 1 m or less; otherwise the trees themselves would be uprooted by the waves. Although *K. candel*

was effective in protecting the coast from erosion during a typhoon, *S. caseolaris* is up to 3 times more effective in attenuating waves (Table S2) due to its vertical roots extending into the water column (pneumatophores) that further contribute to wave attenuation. Error bars are included in Fig. S1A to indicate that the observed wave attenuation field data may vary with regard to mangrove species (e.g. *K. candel* vs *S. caseolaris*), tide elevations (e.g. high, mid or low tide) and the type of coastal storm event (e.g. typhoon, cyclone or other tropical storm).

The quadratic regression for wave attenuation by mangroves depicted in Fig. S1A was compared to a linear regression performed on the same data. The quadratic relationship displayed a better fit (i.e. higher R^2), and the *t*-test for the quadratic term was statistically significant at the 1% level. Thus the quadratic relationship is preferred to the linear regression.

Fig. S1B <u>Salt Marsh</u>

Marsh wave attenuation data was collected in a macro-tidal (mean spring tidal range of 4.8 m) marsh near Tillingham on the Dengie Peninsula, Essex, UK (*S2*). The marshes in this area are near-horizontal and tend to form a narrow (700 m maximum) fringe along the shore. Unvegetated mudflats extend up to 4 km offshore of the marsh edge, and at the study site, a shore-normal mud mound separates the marsh from the mudflat. Wave measurements were made along three transects using Druck (PTX1830) pressure transmitters which recorded wave bursts of approximately 19 min at a 4 Hz frequency during 15 high tides. The data was then Fast-Fourier transformed to obtain significant wave height. Error bars represent variability found in the 15 tides sampled.

The exponential regression for wave attenuation by marshland depicted in Fig. S1B was a significantly better fit (i.e R^2) than a linear regression performed on the same data. In addition, a

McKinnon-White-Davidson *J*-test of the two functional forms indicates that the linear model could be rejected at the 5% confidence level whereas the exponential regression transformed into a log-linear relationship could not be rejected. Thus the exponential regression is preferred to the linear alternative.

Fig. S1C <u>Seagrass Bed</u>

Wave parameters were measured in a *Ruppia maritima* bed off Bishop's Head Point in Chesapeake Bay, Maryland in June 2000 when plants were flowering, plant density was 1,270 ± 92 shoots m^{-2}, and seagrasses occupied most of the water column (1 m). Leaves were approximately 1.5 mm wide. A wave gauge (MacroWave, Coastal Leasing) deployed at 1 m depth within the vegetation was used to record pressure data hourly (4,096 points) at a 5Hz frequency over 14 days (non-storm conditions). The data was Fast-Fourier transformed using Wizard (Coastal Leasing) to obtain wave parameters. Significant wave height was then plotted as a function of water depth, i.e. tidal height. Note that seagrasses occupied most of the water column at all times. During low tide, plant biomass is compressed into a smaller volume of water leading to lower wave heights. Error bars represent variability found in the 24 burst recorded daily for 14 days. Other wave data from the same site can be found in (*S3*-*S5*).

The semi-log regression for wave attenuation by seagrass depicted in Fig. S1C was a significantly better fit (i.e R^2) than a linear regression performed on the same data. In addition, the *J*-test of the two functional forms indicates that the linear model could be rejected at the 5% confidence level whereas the semi-log relationship could not be rejected. Thus the semi-log regression is preferred over the linear alternative.

Fig. S1D Coral Reef

(*S6*) examined the relationship between wave processes and the morphology of nearshore coral reefs under non-storm conditions at numerous sites in Australia. The data presented in Fig. 2D was collected at Warraber Island in the Torres Straight region. The reef platform is 5 km long and has a maximum width of 2.5 km. Mean spring tidal range is approximately 2.4 m. A S4 current and pressure sensor (InterOcean) recorded continuously at a 2Hz frequency in the reef flat basin protected by the reef platform. Estimates of significant wave height were obtained using the standard deviation of the pressure records. These were then plotted as a function of water depth. Meta-Win data extraction program (Sinauer Associates, Inc.) was then used to extract *x*-*y* scatter data. Extracted data were fit to both linear and exponential regression models using JMP statistical software, with the exponential model providing the best fit and greatest reduction in error (i.e., R^2) in comparison to models using only the mean of *x* to predict *y* values. Although a *J*-test of the linear versus exponential regressions is inconclusive, a Box-Cox transformation performed on the linear model indicates that the latter relationship is rejected. Thus the exponential regression is preferred over the linear alternative.

Figure S1E. Sand Dune

Storm wave heights needed to overtop coastal dunes with different amounts of dune grass cover were calculated for the Oregon coast, USA, using sand accumulation data for the European beach grass, *Ammophila arenaria,* (*S7*), introduced to the Pacific coast in the early 1900s, and the total water level modeling approach of (*S8*). Beach grasses trap and accumulate sand in proportion to their density. (*S7*) quantified the relationship between *A. arenaria* growth via lateral dispersion (i.e. percent cover) and sand accumulation (dune height, m) for grass grown on

an unvegetated beach in France over an 8-year period (Table S2). Significant wave heights (H_0) needed to overtop dunes of different heights during the 2% strongest storm events were calculated by comparing estimates of the total water level (TWL) with the elevation of the dunes. Estimates of the TWL achieved on beaches are taken as a combination of tidal level (including storm surge), Z_T, and the two percent exceedence value of wave runup, $R_{2\%}$ for individual swash events.

$$TWL = Z_T + R_{2\%}$$

When the TWL reaches or exceeds the dune height, overtopping, and possibly coastal flooding will occur.

We back calculated significant wave heights (H_o) needed to overtop dunes of different heights using the empirical relationship for wave runup of (*S9*), applicable on natural beaches typical of the Oregon coast (*S10*). The TWL can then be taken as:

$$TWL = Z_T + 1.1\left(0.35\tan\beta(H_0L_0)^{1/2} + \frac{\left[H_0L_0(0.563\tan\beta^2 + 0.004)\right]^{1/2}}{2}\right)$$

Where:

Z_T = MHW + storm surge (assumed here to be linearly dependent and 10% of the storm wave height).

β = typical foreshore beach slope = 1/40

H_0 = offshore significant wave height

$L_0 = \frac{gT^2}{2\pi}$ = offshore wave length

T = typical wave period = 11 seconds

g = acceleration due to gravity = 9.81 m/s^2

Significant wave heights that lead to wave runups that overtop dunes 2% of the time were then plotted against the *A. arenaria* density (which produces dune growth to the heights specified in Table S2) using JMP statistical software. An exponential curve best fit the data with a p-value < 0.0001, which compared more favorably (i.e. R^2) than a linear regression performed on the same data. In addition, the *J*-test of the two functional forms indicates that the linear model could be rejected at the 5% confidence level whereas the exponential regression transformed into a log-linear relationship could not be rejected. Thus the exponential regression is preferred over the linear alternative.

Fig. 1A

For Fig.1A in the article, the net present value (NPV) per km^2 for commercial shrimp farming over a 20-year time horizon and 10% discount rate is based on (*S11*) updated to 1996 US dollars ($); this amounts to a value of $963,227 per km^2. The value of wood products is based on net income per km^2 from mangrove forests to local community (from *S11*, updated to 1996$) of $10,149; over a 20-year time horizon and a 10% discount rate this yields a NPV of $86,405 per km^2. The value of habitat-fishery linkages is based on a net value per km^2 (from *S12*, 1996$, assuming a price elasticity for fish of -0.5) of mangrove habitat of $24,870; over a 20-year time horizon and a 10% discount rate this yields a NPV of $211,729 per km^2. The value of coastal protection from storms is based on a marginal value per km^2 of damages avoided (from *S13*) using the expected damage cost method of $187,898; over a 20-year time horizon and a 10% discount rate this yields a NPV of $1,599,684 per km^2.

Fig. 1B

The various benefits from Fig.1A are assumed to be distributed among the three stakeholder groups in the following way: The mangrove-dependent coastal community is the local community living nearby the mangroves and is dependent on wood products from the mangrove forests, fisheries that benefit from the mangroves as nursery grounds, and the coastal protection from storms provided by the mangroves. The wider coastal community consists of coastal populations living within 5 km inland from the mangroves and benefits from the storm protection value of mangroves only. The outside investors are absentee owners of shrimp ponds created from converting the mangrove ecosystem and are assumed to reside at least 5 km away; they are interested only in the commercial profits of their aquaculture investment.

Fig. 2A

The wave attenuation relationship of Fig. S1A was transformed into a proportionate change in wave height $(y_i - y_0)/y_0$ as a function of each 100 m inshore mangrove distance (see supplementary Fig. S2 below), where y_i is from Fig S1A and $y_0 = 1.1$. The resulting relationship in Fig. S2 was used to adjust the net present value per km^2 estimate for storm protection employed in Fig. 1A, assuming that each km^2 of mangroves deforested involved the equivalent loss of 100 m mangroves inshore along the 10 km coastline. Fig. S2 assumes that the mangrove consists of the species *Kandelia* and that the wave occurs at mid-tide. With no mangroves (distance 0 m) it is assumed that the wave has a maximum height of 1.1 m. Table S3 displays the calculations corresponding to how the proportionate change in wave height of Fig. S2 was used to adjust the net present value per km^2 for the coastal protection service. In Table S3 it is assumed that every additional 1 km^2 of mangrove along the coastline is equivalent to an

additional area of forest consisting of 100 m inshore along the 10 km shoreline (e.g. 100 m x 10,000 m). The formula for the value estimates in Table S3 (for any km^2 of mangrove > 0) is therefore $V(M_i) = V(M_{i-1}) + \left[(\$1{,}599{,}684) * (W(x_i) - W(x_{i-1})) * 10\right]$. For example, the storm protection value of a mangrove area of 4 km^2 is $V(4)$ = \$7,149,601 + [(\$1,599,684)*(0.5532 - 0.4469)*10) = \$8,849,953.

Fig. 2B

The various benefits from Fig. 2A are assumed to be distributed among the three stakeholder groups in the same way as in Fig. 1B.

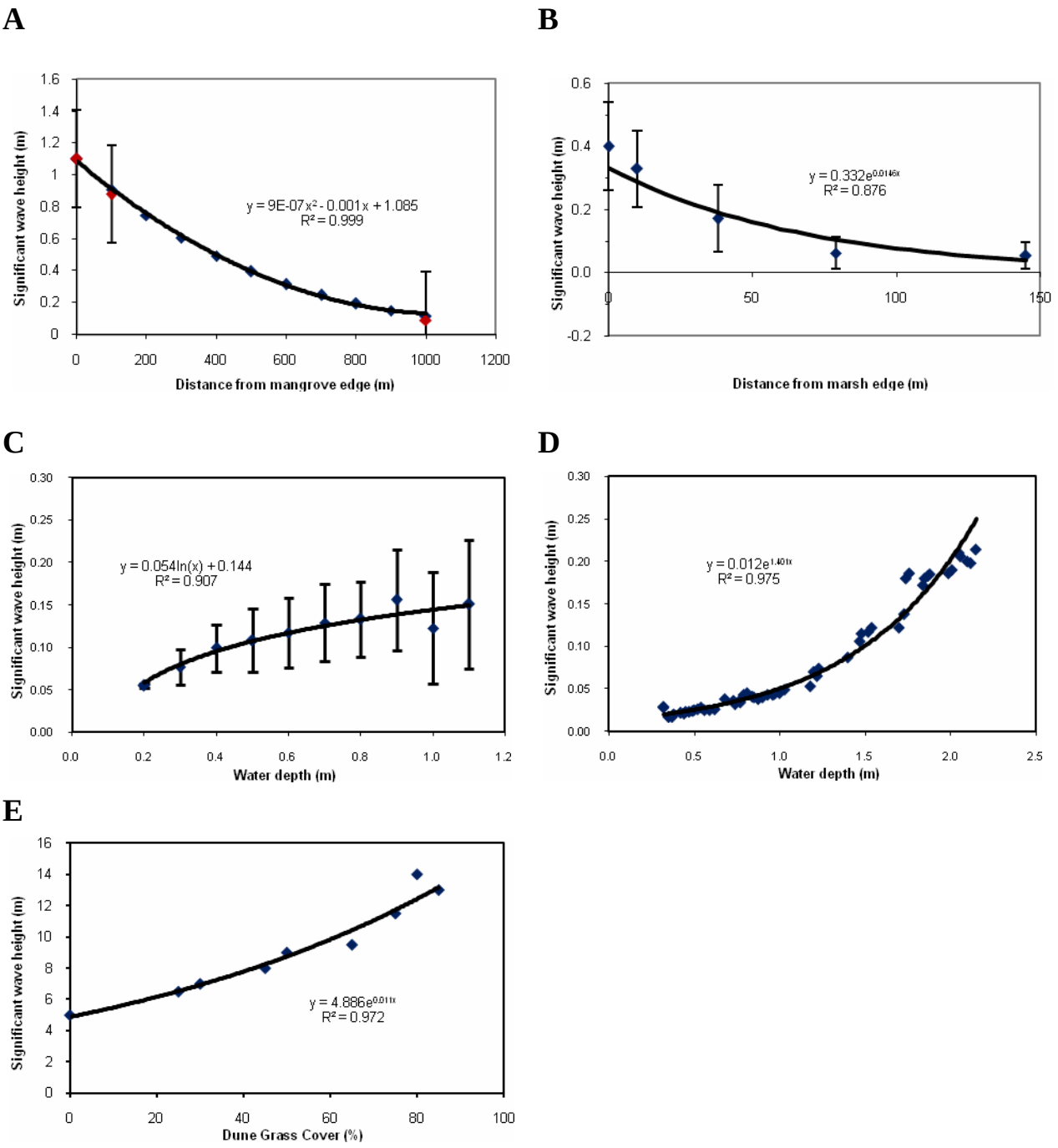

Fig. S1 Wave attenuation by (**A**) mangroves in terms of wave height (m) affected by distance of mangroves inland from seaward edge, by (**B**) marshland in terms of wave height (m) affected by distance of marsh inland from seaward edge, by (**C**) seagrass in terms of wave height (m) affected by surface water depth (m) above sediment surface, by (**D**) near-shore coral reef in terms of wave height (m) affected by surface water depth (m) above coral reef, and by (**E**) wave height (m) exceeding dune affected by percentage of grass to total dune area.

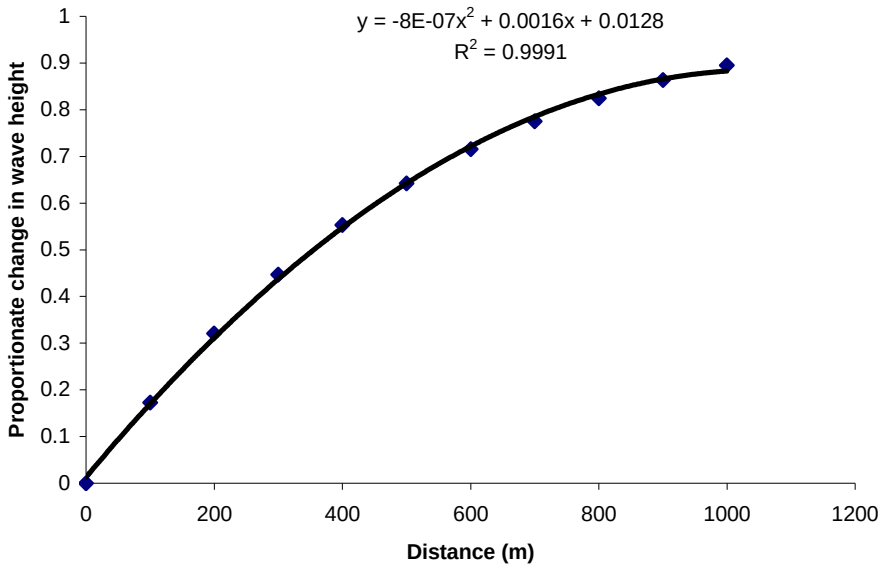

Figure S2. Proportionate change in wave height at mid-tide as a function of 100 m inshore *Kandelia* mangrove distance (from Fig. S1A)

Table S1. Wave reduction (*r*, in %) per 100 m of adult mangrove plantation (data from *S1*). The value of r without mangroves was about 5% next to the *Kandelia candel* site and 10% next to the *Sonneratia caseolaris* site.

Water depth (m)	**0.2**	**0.4**	**0.6**	**0.8**
Kandelia candel	20	20	18	17
Sonneratia caseolaris	60	40	30	15-40

Table S2. Significant wave height (H_0) that leads to a wave runup that overtops dunes (2% of the time) with different plant (*Ammophila arenaria)* densities. Note that, as *A. arenaria* density increases over time, dune height also increases due to sand deposition. As a result, higher waves are needed to overtop the dune. Plant and dune data from (*S7*).

Time Since Planted (yrs)	Plant density (% cover)	Dune Height (m)*	Ho (m)
1	25	2.25	6.5
2	30	2.4	7
3	45	2.6	8
4	50	2.75	9
5	65	2.9	9.5
6	75	3.25	11.5
7	85	3.6	13
8	80	3.75	14

*all values adjusted by +2m from values in (*S7*) to include average elevation above maximum height of wave (MHW) to the top of the dune (based on Oregon beaches).

Table S3. Non-linear estimates of coastal protection service of mangroves (*Kandelia candel*).

Mangrove area, km^2 (M_i)	**100 m inshore mangrove distance (x_i)**	**Proportionate change in wave height $W(x_i)$**	**Value of coastal protection service, \$ $V(M_i)$**
0	0	0	\$0
1	100	0.1726	\$2,760,546
2	200	0.3208	\$5,131,977
3	300	0.4469	\$7,149,601
4	400	0.5532	\$8,849,953
5	500	0.642	\$10,269,517
6	600	0.7154	\$11,443,689
7	700	0.7755	\$12,405,983
8	800	0.8244	\$13,187,464
9	900	0.8637	\$13,816,385
10	1000	0.8951	\$14,317,997

Supporting references

S1. Y. Mazda, M. Magi, M. Kogo, P.N. Hong, *Mangroves and Salt Marshes* **1**, 127-135 (1997).

S2. I. Möller, *Estuarine, Coastal and Shelf Science* **69**, 337-351 (2006).

S3. R. Newell, E. Koch, *Estuaries* **27**, 793-806 (2004).

S4. E. Koch, L. Sanford, S.-N. Chen, D. Shafer, J. Smith, 2006. "Waves in seagrass systems: review and technical recommendations." (US Army Corps of Engineers Technical Report. Engineer Research and Development Center, ERDC TR-06-15, Washington, DC, 2006).

S5. S.-N.Chen, , L. Sanford, E. Koch, F. Shi, E. North, *Estuaries* **30**, 296-310 (2007).

S6. P. Kench, R. Brander, *Journal of Coastal Research* **22**, 209-223 (2006).

S7. F. Roze, S. Lemauviel, *Restoration Ecology* **12**, 29-35 (2004).

S8. P. Ruggiero, P. Komar, W. McDougal, J. Marra, R. Beach. *Journal of Coastal Research* **17**, 407-419 (2001).

S9. H. Stockdon, R. Holman, P. Howd, A. Sallenger, *Coastal Engineering* **53**, 573-588 (2006).

S10. P. Ruggiero, G. Kaminsky, G. Gelfenbaum, B. Voigt, *Journal of Coastal Research* **21**, 553-578 (2005).

S11. S. Sathirathai, E. Barbier, *Contemporary Economic Policy*, **19**, 109-122 (2001).

S12. E. Barbier, *Contemporary Economic Policy* **21**, 59-77 (2003).

S13. E. Barbier, *Economic Policy* **22**, 177–229 (2007).